Asian Journal of Chemistry; Vol. 24, No. 10 (2012), 4579-4582

ASIAN JOURNAL OF CHEMISTRY

www.asianjournalofchemistry.co.in

Core/Shell and Multi-Scale Structures Enhance the Electrocatalytic Oxygen Reduction Reaction of the PdSn@Graphene Nano-Composites in an Alkaline Condition

WENZHAO GONG[1,2,*], CHENGMENG CHEN[1,2], QINGQIANG KONG[1,2], MAO-ZHANG WANG[1], YUE-FANG WENY[1], LANG LIU[1] and YONGGANG YANG[1]

[1]Key Laboratory of Carbon Materials, Institute of Coal Chemistry, Chinese Academy of Sciences, Taiyuan 030001, P.R. China
[2]Graduate University of Chinese Academy of Sciences, Beijing 100049, P.R. China

*Corresponding author: E-mail: gangwenzhao@163.com

(*Received*: 12 August 2011; *Accepted*: 9 May 2012) AJC-11441

The core/shell electrocatalyst of PdSn nanoparticles supported on graphene was reported. Morphology, crystallinity and elements content of the synthesized materials were investigated by X-ray diffraction (XRD), transmission electron microscope (TEM) and energy dispersive X-ray (EDX), respectively. The results showed that the graphene support highly and homogeneously dispersed PdSn nanoparticles at the different soaking times. Catalyst activity for oxygen reduction reaction in an alkaline condition was investigated by cyclic voltammetry (CV). The fundamental electrochemical test results indicated that PdSn@graphene nano-composites could be considered a much better electrocatalyst material for use in alkaline fuel cell cathode materials.

Key Words: PdSn@Graphene, Nano-composites, Oxygen reduction reaction.

INTRODUCTION

Recently, there has been a resurgence of interest in alkaline fuel cells (AFCs) because of the development of alkaline anion exchange membranes[1] and the utilization of non-Pt metal catalysts[2]. The electrocatalytic oxygen reduction reaction (ORR) has attracted extensive interest due to its importance in the fuel cells[2-4]. A high metal dispersion[5-7] is an important design factor for oxygen reduction reaction catalysts not only in alkaline fuel cells but also in acid-based polymer electrolyte membrane fuel cells (PEMFCs) because it conserves expensive metals such as Pt[5-9].

As a single-atom-thick carbon material with light weight and high surface area and conductivity, graphene[10,11] could be an ideal substrate for growing and anchoring of functional nanomaterials for high-performance electrocatalytic or electrochemical devices. It has attracted great interest from many researchers in recent years to decorate nanoparticles on graphene, such as Sn, Pt, Ni, Pd and so on[12-17]. Pt/graphene and Pd/graphene electrocatalysts have been reported to use as anode and cathode electro-catalysts for hydrogen oxidation and oxygen reduction reactions, respectively[15-17].

In this work, graphene are used as an excellent support to synthesize small and uniformly dispersed PdSn nanoparticles. The particle size, size distribution and structural information are verified using transmission electron microscopy (TEM), energy dispersive X-ray (EDX) and X-ray diffraction (XRD). The active oxygen reduction reaction performance of graphene-supported PdSn catalysts (PdSn/graphene nano-composite) with highly dispersed catalyst particles are described in alkaline solutions employing the cyclic voltammetry (CV).

EXPERIMENTAL

Synthesis of electrocatalyst: The graphene used in this study was prepared by rapid thermal expansion of graphene oxide that had been made according to the modified Hummers method.

The as-prepared graphene (10 mg) was dispersed *via* ultrasonication in 100 mL of 5 % wt sodium dodecyl sulfonate (SDS) water solution. An aqueous solution (0.1 M of $SnCl_2$/0.1 M of HCl) was immersed and ultrasonication at 25 ºC for 0.5 h, followed by washing with de-ionized water. After washed, Sn@graphene was vigorously refluxed in the aqueous mixture of 0.0014 M of $PdCl_2$ and 0.25 M of HCl at 25 ºC in 10, 20, 30 and 60 min, respectively, with ultrasonication.

Prepatation of catalyst electrode: The working electrodes were prepared by mixing mass fraction 90 % PdSn@graphene material and 10 % polytetrafluoroethylene (PTFE) in 7 mL ethanol followed by an ultrasonication treatment for 20 min. The slurry of the mixture was put onto a nickel foam current collector with an area of 1 cm^2 and pressed under a pressure of 10 MPa for 5 min to fabricate an electrode. The performance

of a single electrode was tested on CHI760D electrochemical workstation. The cyclic voltammetric experiments were carried out at room temperature under flowing nitrogen with a convention active three-electrode electrochemical setup, in which the active materials electrode served as working electrode and a platinum plate and Hg/HgO were used counter electrode and reference electrode, respectively. 0.1 M NaOH was used as the electrolyte.

RESULTS AND DISCUSSION

Characterization of Sn-Pd/graphene: The morphologies and structrural features of the as-prepared PdSn@ graphene nano-composites are shown in Fig. 1(a-d). It is clear that catalyst nano-particles are highly and homogeneously dispersed on the surface of graphene. As ultraphonic time prolonged, the diameter of nano-particles can be observed to increase from Fig. 1(a-c). The PdSn nano-particles are generally between 1 and 2 nm in diameter after the 10 min of soaking (Fig. 1a), while after the 1 h of soaking are between 5 and 10 nm (Fig. 1c). And these nano-particles cumulate with each other. The cross-sectional high-magnification TEM image of Fig. 1(d) shows that PdSn nano-particle has a polycrystalline structure. The crystal domains with PdSn nano-particle have an interfringe distance of 0.3794 nm, which is close to the Pd crystal (0.389).

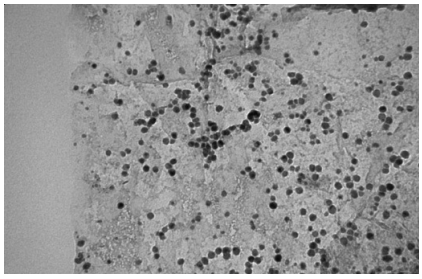

(a)

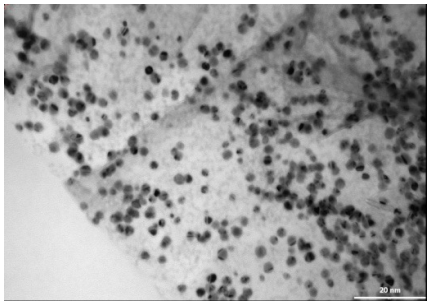

(b)

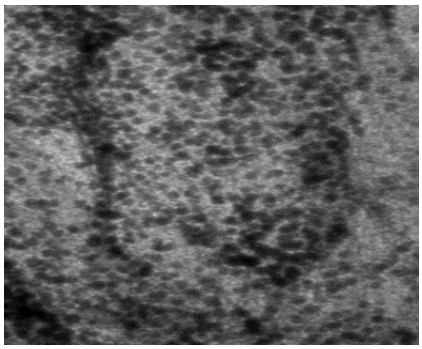

(c)

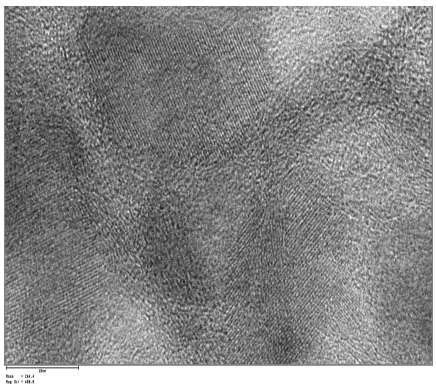

(d)

Fig. 1. TEM image of the PdSn@Pt/graphene nano-composites (a, b, c corresponding with the soaking time of 10, 20 and 60 min), (d) the cross-sectional high-magnification TEM image of the 20 min soaking time of graphene nano-composite

The value was in good agreement with the XRD data. In addition, the EDX patterns in Fig. 2 reveal that PdSn@graphene catalysts were composed of C, Sn and Pd elements (refer to the EDX spectrum in Fig (b-d), a Cu holey carbon support grid was used).

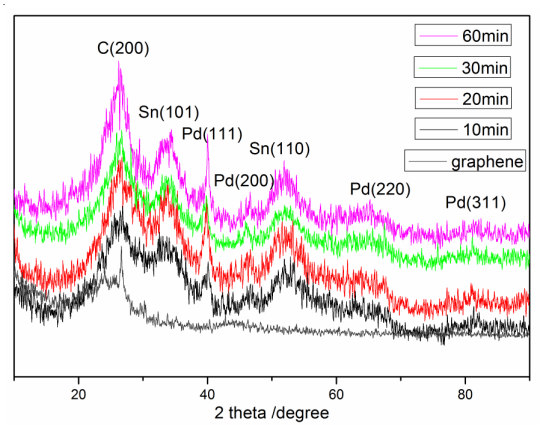

Fig. 2. XRD patterns of the bare graphene and PdSn@ graphene nano-composites

Fig. 2 shows the XRD patterns of PdSn@graphene nano-composites. The peak about at 2θ = 24.8º all XRD patterns corresponds to the (200) plane of the graphene support (Fig. 2a). The peaks about at 2θ = 33.81º and = 51.6º are indicative of the formation of Sn. The other four peaks are characteristics of the face-centred cubic (fcc) crystallite Pd for planes (111), (200), (220), (311).

The composition analysis of the PdSn@graphene nano-composites was performed by EDX. Prolonged the time of impregnation, it was found that the metal ration of Pd was increased dramatically. The reason why the Sn would be reduced and then cover the PdSn particles could be attributed to (i) the interaction between the metals would be stronger than that between metal and graphene; (ii) Pd crystallite and Sn are all with fcc structure, which is in favour of the epitaxial growth of the Pd shell on the Sn core; (iii) As the replacement reaction takes place, the Sn atom on the surface of graphene are easily oxidised to Sn^{X+} and the Pd^{2+} reduced to Pd. Consequently, the catalyst surface will be covered with the Pd. This

core-shell structure can improve the performance of oxygen reduction reaction, which will be as follows.

Electrocatalytic properties of Sn-Pd/graphene: The cyclic voltammetry of the oxygen reduction reaction on graphene and different soaking time of PdSn@graphene nano-composites shown in Fig. 4, which were recorded in 0.1 M NaOH alkaline solutions. Fig. 4(a) shows the oxygen reduction reaction for these catalysts with the scan rate of 10 mVs^{-1}. The oxygen reduction reaction peaks were present at E = 0.48 V, whereas the oxygen reduction reaction peak of curve b was E = 0.465 V. In Fig. 4(b), the onset potential of oxygen reduction reaction was observed at 0.401 V on curve blank, at 0.377 V on curve a, at 0.31 V on curve b, at 0.373 V on curve c and at 0.385 V on curve d, indicating the oxygen reduction reaction on PdSn@graphene nano-composites could proceed at lower potential. The peak potential shifted negatively with increasing Pd atomic ratio but the peak current increased with the soaking time until 20 min and then decreased for PdSn nanoparticles catalyst. It could be seen that catalyst with Pd:Sn atomic ratio of 1:1 had the highest oxygen reduction reaction activity, according to the EDX data of Fig. 3(c).

This indicate that the catalytic mechanism of PdSn@graphene nano-composites for oxygen reduction reaction might be the same as Pd. The electrocatalytic activity enhancements for oxygen reduction reaction are considered that (i) PdSn@graphene nano-composites have a larger surface area than the bare graphene, which provides more active sites and results in high electrocatalytic activity; (ii) core-shell nanostructure increases the utilization efficiency of precious metal electrocatalysts and (iii) the electronic effect between Sn and Pd.

Besides, due to diffusion limitations of O_2 into the micropores of graphene aggregates, a large portion of the PdSn nanoparticles embedded deeply in the aggregated restacked graphene structure are most likely not available for the oxygen reduction reaction. Oxygen diffusion within such micropores should not be strongly affected by hydrodynamic conditions, *i.e.*, the increasing Pd atomic ratio should have nagetive effect into the diffusion of O_2 into micropores with long diffusion length. This will explain the observation of the potential variations in Fig. 4(b). As the O_2 diffusion path will be longer for larger sized graphene, the amount of inactive PdSn nanoparticles for the oxygen reduction reaction will increase. In other words, only PdSn nanoparticles near the edges of graphene are electrochemically active for oxygen reduction reaction. The decrease in specific activity with the increase in Pd atomic ratio is in agreement with the above assumption. The results obtained in this work clearly illustrate the importance of the Pd content of PdSn@graphene nano-composites for full utilization of the electrocatalyst.

Conclusion

In summary, we showed that the PdSn@graphene nanocomposite can be synthesized in solution with graphene as the substrate and uniformly dispersed core-shell PdSn nanoparticles were successfully deposited on the graphene. The results were discussed in terms of the slow O_2 diffusion through the micropores of aggregated graphene. The importance of the structure of the Pd content of PdSn@graphene nano-composites for full utilization of the electrocatalyst has

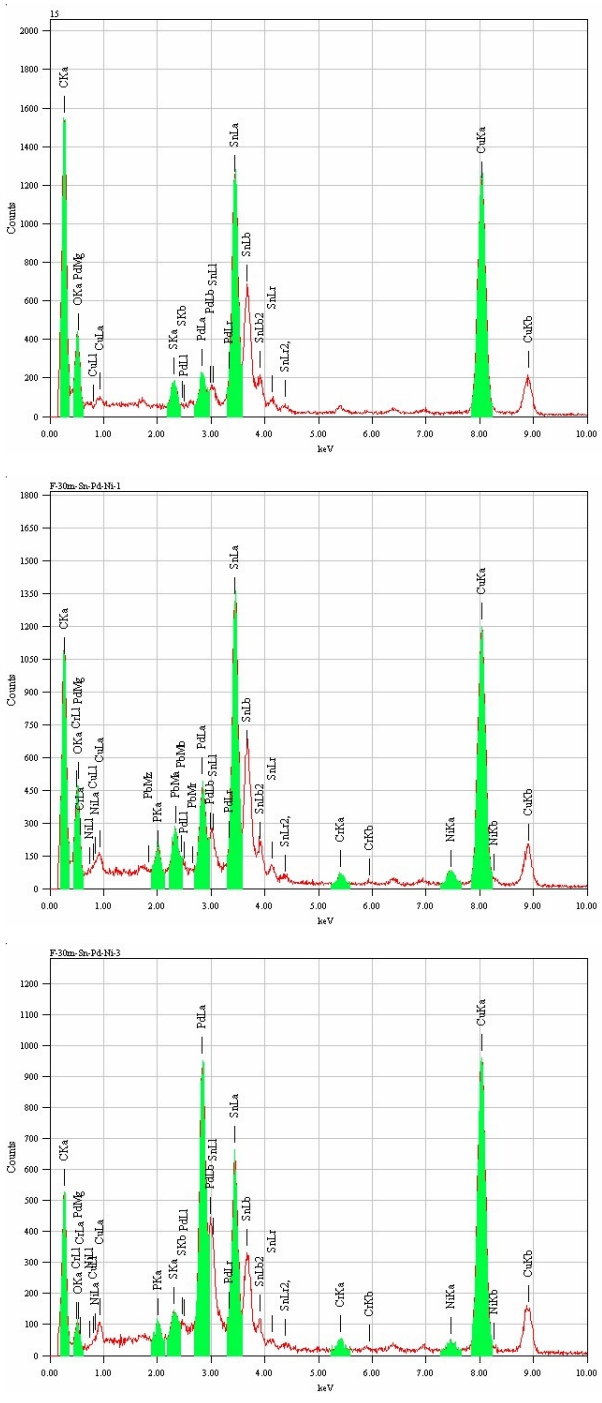

Fig. 3. Composition analysis of the PdSn@graphene nano-composites by EDX a, b and c are corresponded to the soaking time of 10, 20 and 60 min

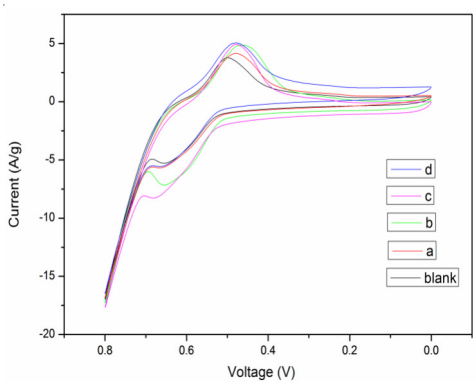

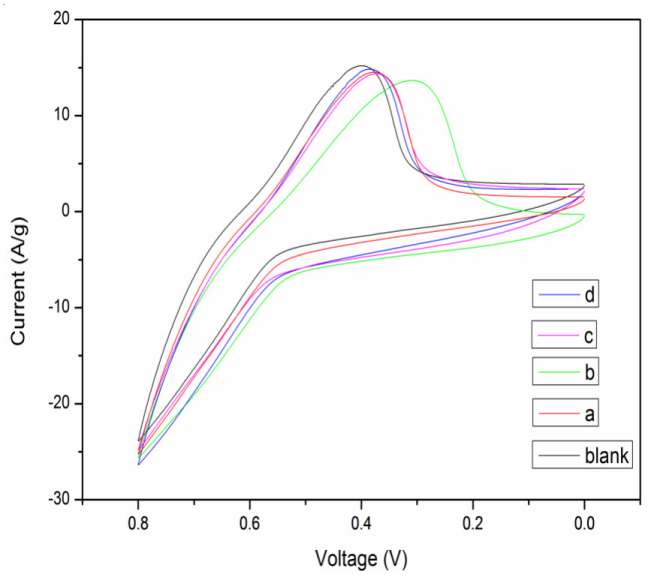

Fig. 4. Cyclic voltammetric curves of the scan rate of 10 mV s^{-1} (a) and 100 m V^{-1} (b) (a, b, c, d and blank *versus* the impregnated time of 10, 20, 30 and 60 min and the bare graphene)

been demonstrated. These results suggest that PdSn@graphene nano-composites could be considered a good electrocatalyst material for use in alkaline fuel cell cathode materials.

REFERENCES

1. J.S. Park, S.H. Park, S.D. Yim, Y.G. Yoon, W.Y. Lee and C.S. Kim, *J. Power Sources*, **178**, 620 (2008).
2. F. Bidault, D.J.L. Brett, P.H. Middleton and N.P. Brandon, *J. Power Sources*, **187**, 39 (2009).
3. J. Guo, A. Hsu, D. Chu and R. Chen, *J. Phys. Chem. C*, **114**, 4324 (2010).
4. H.J. Kim, Y.S. Kim, M.H. Seo, S.M. Choi, J.M. Cho, G.W. Huber and W.B. Kim, *Electrochem. Commun*., **12**, 32 (2010).
5. K.J.J. Mayrhofer, D. Strmcnik, B.B. Blizanac, V. Stamenkovic, M. Arenz and N.M. Markovic, *Electrochim. Acta*, **53**, 3181 (2008).
6. J. Perez, E.R. Gonzalez and E.A. Ticianelli, *Electrochim. Acta*, **44**, 1329 (1998).
7. M.H. Seo, S.M. Choi, H.J. Kim, J.H. Kim, B.K. Cho and W.B. Kim, *J. Power Sources*, **179**, 81 (2008).
8. A. Peigney, C. Laurent, E. Flahaut, R.R. Bacsa and A. Rousset, *Carbon*, **39**, 507 (2001).
9. M.H. Seo, S.M. Choi, H.J. Kim and W.B. Kim, *Electrochem. Commun.*, **13**, 182 (2011).
10. A.K. Geim and K.S. Novoselov, *Nature Mater*., **6**, 183 (2007).
11. X.L. Li, X.R. Wang, L. Zhang *et al*., *Science*, **319**, 1229 (2008).
12. W. Zhang, R. Wang, H. Wang and Z. Lei, *Fuel Cells*, **10**, 734 (2010).
13. Y.C. Zhao, L. Zhan, J.N. Tian, S.L. Nie and Z. Ning, *Electrochim. Acta*, **56**, 1967 (2011).
14. R.Z. Hu, H. Liu, M.Q. Zeng, H. Wang and M. Zhu, *J. Mater. Chem*., **21**, 4629 (2011).
15. J. Sato, K. Higurashi, K. Fukuda and W. Sugimoto, *Electrochemistry*, **5**, 337 (2011).
16. Q.L. Yue, K. Zhang, X.M. Chen, L. Wang, J.S. Zhao , J.F. Liu and J.B. Jia, *Chem. Commun*., **46**, 3369 (2010).
17. K. Zhang, Q. Yue, G. Chen, Y. Zhai, L. Wang, H. Wang, J. Zhao, J. Liu, J. Jia and H. Li, *J. Phys. Chem. C*, **115**, 379 (2011).